meant to represent standard deviations in the measurement and do *not* include the possible systematic error in the optical measurement corresponding to different values of f which could cause the values of $\mathcal{P}_3$ and their errors to be multiplied by a single factor between 0.85 and 1.15 as discussed previously.

The errors quoted in the incident proton energies arise from an estimate of the accuracy of the accelerator calibration and the determination of the energy loss in the entrance foil of the target.

Phase-shift searches incorporating these data have been presented by Haeberli and Morrow[6] and need not be described here. It is sufficient to say that these authors have found that two different families of phase shifts, the one found by them and the one found by Tombrello,[3] can be adjusted to include these data.

A subsequent experiment[7] has allowed a more precise specification of the phase shifts in the neighborhood of 9-MeV proton energy and the results of further phase-shift analyses are presented with the report of that work.

ACKNOWLEDGMENTS

We would like to thank Professor G. C. Phillips, Professor G. K. Walters, Professor M. Tanifuji, and Dr. L. D. Schearer for their interest and help in this work, and Professor W. Haeberli and Dr. Roy Morrow for giving their results to us in advance of publication.

PHYSICAL REVIEW VOLUME 178, NUMBER 4 20 FEBRUARY 1969

Proton-Proton Bremsstrahlung at $E_p = 10$ MeV*

A. NIILER,† C. JOSEPH,‡ V. VALKOVIC,§ R. SPIGER, T. CANADA, S. T. EMERSON, J. SANDLER, AND G. C. PHILLIPS
T. W. Bonner Nuclear Laboratories, Rice University, Houston, Texas 77001

(Received 26 August 1968)

A measurement of the proton-proton bremsstrahlung cross section at $E_p = 10$ MeV has been made. Two silicon surface-barrier detectors were placed in a hydrogen gas target at 30° on opposite sides of the beam axis. The energies of the two final-state protons and their time-of-flight difference were measured. E_1-E_2 spectra corresponding to events in the true and accidental regions of the time spectrum were obtained in off-line analysis. An upper limit of 0.42 μb/sr^2 has been established for the proton-proton bremsstrahlung cross section at $E_p = 10$ MeV, $\theta = 30°$.

INTRODUCTION

CONSIDERABLE effort has been spent recently in the calculation[1–5] and measurement[6–11] of the nucleon-nucleon bremsstrahlung cross section over an energy range of 10–200 MeV. It was hoped, at the beginning of this period of activity, that the off-energy shell behavior of the nucleon-nucleon bremsstrahlung process might lead to the determination of an unambiguous model of the nucleon-nucleon potential. However, several potentials predict quite closely the bremsstrahlung cross section over the energy range. Probably the best fits to data have been obtained by Pearce *et al.*[3] using the Tabakin nonlocal, separable potential, and by Brown[4] using the Bryan-Scott one-boson-exchange potential. A comparably good fit has been obtained by Brown with the Hamada-Johnston potential. Finally, Signell[5] and Nyman[12] have shown that the potential model-dependent contribution to the proton-proton bremsstrahlung cross section is small compared to the model-independent part.

By far the largest amount of work has been done on the proton-proton bremsstrahlung (PPB hereafter), although the neutron-proton process has received some attention.[3,7] All of the PPB data, except for one case,[13] have been at an incident energy above 20 MeV. Complete calculations have not been extended below 20 MeV since some of the approximations used for the higher energy calculations are no longer valid. It is

* Work supported in part by the U.S. Atomic Energy Commission.

† Present address: Los Alamos Scientific Laboratory, Los Alamos, N.M.

‡ Present address: Institut de Physique Nucléaire, Lausanne, Switzerland.

§ Present address: Institut "Ruder Boxkovic," Zagreb, Yugoslavia.

[1] J. Ashkin and R. E. Marshak, Phys. Rev. **76**, 58 (1949).
[2] A. H. Cromer and M. I. Sobel, Phys. Rev. **152**, 1351 (1966).
[3] W. A. Pearce, W. A. Gale, and I. M. Duck, Nucl. Phys. **B3**, 241 (1967).
[4] V. R. Brown, Phys. Letters **25B**, 506 (1967).
[5] P. Signell, in *Proceedings of Symposium on Light Nuclei, Few Body Problems, and Nuclear Forces*, edited by I. Slaus and G. Paic (Gordon and Breach Science Publishers, Inc., New York, 1969).
[6] B. Gottschalk, W. J. Shlaer, and K. H. Wang, Nucl. Phys. **A94**, 491 (1967).
[7] K. W. Rothe, P. F. M. Koehler, and E. H. Thorndike, Phys. Rev. **157**, 1247 (1967); Bull. Am. Phys. Soc. **11**, 303 (1966).
[8] I. Slaus, J. W. Verba, J. R. Richardson, R. F. Carlson, W. T. H. Van Oers, and L. S. August, Phys. Rev. Letters **17**, 536 (1966).
[9] R. E. Warner, Can. J. Phys. **44**, 1225 (1966).
[10] M. L. Halbert, D. L. Mason, and L. C. Northcliffe, Phys. Rev. **168**, 1130 (1968).
[11] A. Bahnsen and R. L. Burman, Phys. Letters **26B**, 585 (1968).
[12] E. M. Nyman, Phys. Letters **25B**, 135 (1967); and (private communication).
[13] G. M. Crawley, D. L. Powell, and B. V. Narashima Rao, Phys. Letters **26B**, 576 (1968).

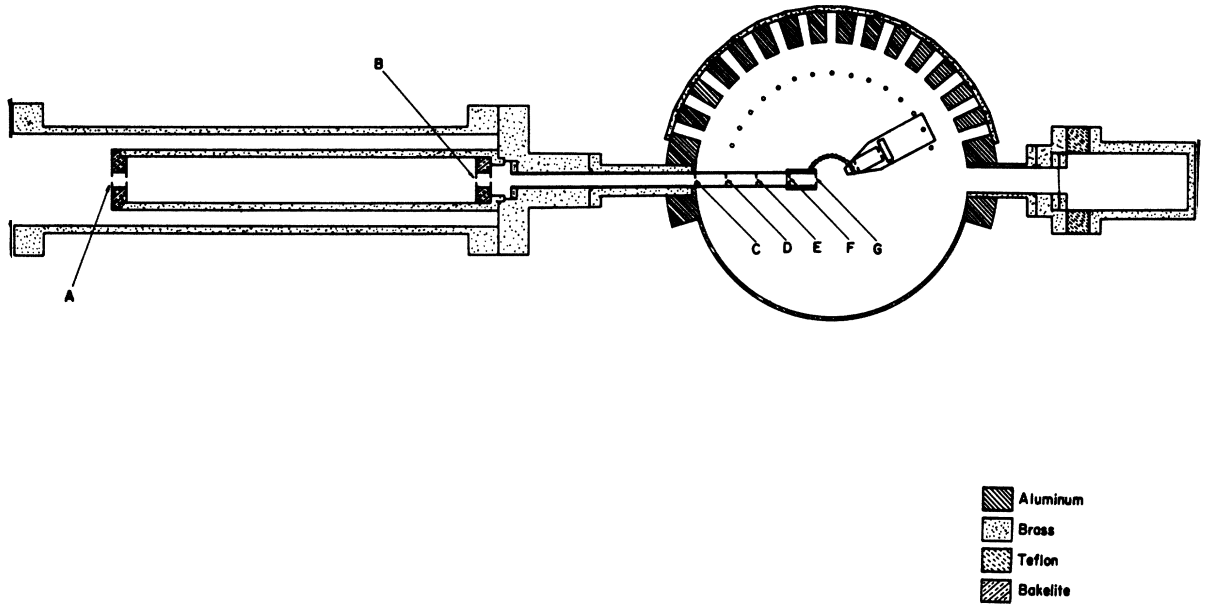

FIG. 1. Plane section of the scattering chamber at the beam line.

apparent, however, from all present data and calculations that σ_{PPB} is monotonically decreasing with decreasing energy and should drop below 1 μb/sr^2 at $E_p=10$ MeV.

APPARATUS AND EXPERIMENTAL METHOD

A. Scattering Chamber

A new chamber, designed specifically for three-body experiments with gas targets, was used in this experiment (see Fig. 1). The incoming beam is collimated by slits A and B, both 1.0 mm in diameter and 30.0 cm apart. Slits C, D, and E (1.1, 1.2, and 1.3 mm in diameter, respectively) are antiscattering slits before the 6250 Å thick nickel entrance foil. Two antiscattering slits of 1.5 and 1.6 mm diameter (F and G) follow the entrance foil. All of the slits, A–G, are of 0.25-mm-thick tantalum. With this collimation system, the beam is constrained to be no more than 1.5 mm in diameter at the chamber center. The chamber wall is cast aluminum, 2.54 cm thick. The aluminum is cut away on one side leaving a 3-mm-thick window covering an angular opening of 140° for experiments in which a final state neutron is to be detected. The aluminum chamber bottom has positioning holes permitting solid-state detectors to be placed at 10° intervals from 20° to 160° on either side of the beam. The rotatable aluminum top allows four solid-state detectors to be mounted at 90° intervals and to be set to continuously variable angles with respect to the beam direction to 0.1° accuracy. The lid rests on a ball race and seals against the inside wall of the chamber by means of a rotating O-ring seal. In case the measurement of a charged particle time of flight is required, port holes at 10° intervals from 20° to 160° on one side of the chamber permit the attachment of an evacuated tube capped by a solid-state detector holder assembly. The beam leaves the chamber through a 2.54-cm-diam hole and a 25 000 Å thick nickel foil into a Faraday cup where it is stopped in a 1.5-mm gold plate. The inside dimensions of the chamber (22.8 cm diam by 5.08 cm height) were kept small in order to allow the use of relatively expensive target gases.

B. Experimental Detail

In the present experiment a 10-MeV proton beam of ~300 nA intensity, obtained from the Rice tandem Van de Graaff accelerator, was incident on a hydrogen gas target at a pressure of 20 cm Hg. Two silicon surface barrier detectors were placed at 30° on opposite sides of the beam axis in what has become known as the Harvard geometry.[6] Both detectors were collimated by two circular tantalum slits, 2.40 mm in diameter and 17.8 mm apart, and subtended horizontal and vertical angles of $\pm 1.27°$ at the center of the target. A diagram of the experimental geometry and electronics is shown in Fig. 2.

A coincident measurement of the energies in the two detectors plus a time difference between their signals was recorded in a $1024\times 1024\times 1024$-channel computer-analyzer system. Windows were set on both detectors such that both the elastic protons and low-energy multiply scattered events were rejected in the three-parameter spectra. The energy range in which events in both detectors were accepted was approximately 1.0 to 6.0 MeV. Since the PPB events are constrained by kinematics to lie between 3.0 and 3.6 MeV, there was no danger of discriminating against these events with these window settings.

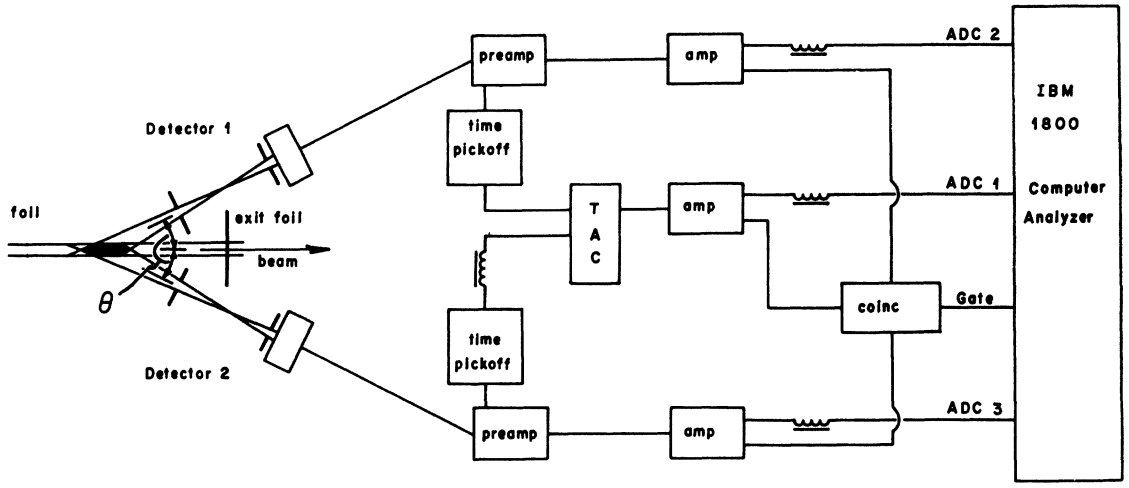

FIG. 2. Schematic diagram of the physical setup and the electronics.

Although no change in the contamination was observed, the target gas was changed every 10 h during the total bombardment time of 72 h. Elastic protons were counted in both detectors. In order to determine the position of the true coincidence peak in the time spectrum, a three-parameter measurement was taken with the detectors 90° apart in the laboratory detecting p-p elastic scattering. This calibration was done over a bombarding energy interval of 3–11 MeV so that the effect of the energy dependence of rise times in the detectors and particle time of flight on the time spectrum could be determined. This measurement also provided a convenient check on the linearity of the energy scales.

ANALYSIS AND DISCUSSION

The data were analyzed off-line by first correcting the time spectrum for detector rise and proton flight times, using the technique of Emerson *et al.*[14] Windows of 20 nsec width were set in the time spectrum about the true coincidence peak position and about another region consisting of background. All three-parameter events which had the time in one of the windows were sorted and plotted in an E_1-E_2 spectrum. The distribution of events in the E_1-E_2 plane is shown in Fig. 3. The events corresponding to the time in the true or foreground window of the time spectrum are shown in Fig. 3(a), and the events corresponding to the time in the background window are shown in Fig. 3(b). The locations of PPB events in this E_1-E_2 plane are uniquely determined by the kinematics of the $p+p\rightarrow p+p+p+\gamma$ reaction and form a well-defined locus. In Fig. 3, the closed solid curves show the PPB locus while the second solid curve gives the locus for breakup protons from the $d(p, 2p)n$ reaction. The dashed curves show the calculated limits of the PPB and breakup proton regions. All events within the dashed curve around the PPB locus are taken to be due to the PPB process. There are 11 counts within the dashed curve in the foreground spectrum and 19 counts in the background spectrum. Including one standard deviation, the net yield of PPB events is thus ≤ 5.5 counts.

Each event in the background spectrum was subtracted from the event nearest to it in the foreground spectrum and the net effect is plotted also in Fig. 4. A number of counts can be observed along the p-d breakup locus since the hydrogen gas contains some deuterium impurity. The yield of these breakup events agrees reasonably well with our previous measurements of this reaction cross section using both gas and thin deuterated polyethylene[15] targets. An exact comparison is not possible, because of the uncertainty in the amount of the deuterium impurity. The hydrogen gas used was produced by a fractional separation method and no deuterium impurity data were available. The net counts near low values of E_1 and E_2 ($\sim$2–3 MeV) and around $E_1=6$ MeV reflect the statistical uncertainty in those regions due to larger backgrounds from elastic protons and multiply scattered particles.

The PPB cross section is calculated from the expression

$$\left(\frac{d^2\sigma}{d\Omega_1 d\Omega_2}\right)_{\mathrm{PPB}} = \frac{N_{\mathrm{PPB}}}{N_{\mathrm{el}}}\left(\frac{d\sigma}{d\Omega}\right)_{\mathrm{el}}\frac{F_1}{F_2}, \qquad (1)$$

where N_{PPB} is the net yield in the region of the PPB locus, N_{el} is the number of elastic protons at 30°, and $(d\sigma/d\Omega)_{\mathrm{el}}$ is the 30° p-p elastic cross sections (190 μb/sr) at 9.74 MeV.[16] F_1 and F_2 are the geometrical factors incorporating the finite beam size and the finite angular

[14] S. T. Emerson, W. D. Simpson, J. C. Legg, and G. C. Phillips, Nucl. Instr. Methods **52**, 229 (1967).

[15] A. Niiler, C. Joseph, V. Valkovic, and G. C. Phillips, Bull. Am. Phys. Soc. **12**, 1174 (1967).

[16] B. Cork and W. Hartsough, University of California Radiation Laboratory Report No. UCRL 2312 (unpublished).

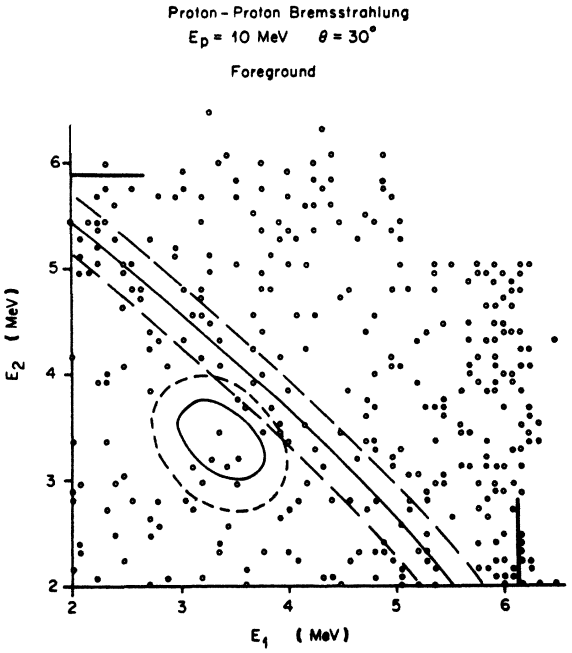

FIG. 3. The PPB kinematics and data at $E_p=10$ MeV, $\theta=30°$. (a) Shows the foreground distribution of events in the E_1-E_2 plane, each dot representing one count. (b) Shows the background distribution of events in the E_1-E_2 plane, each dot representing one count. In both (a) and (b), the solid closed curve is the PPB locus and the other solid curve is the *p-d* breakup locus as calculated from kinematics. The dashed curves are the limits within which events are assigned to the PPB or *p-d* breakup processes. The short, straight solid lines near 6 MeV along each axis show the positions at which windows were placed on the two-energy spectra.

openings of the detector slit systems for a single detector and two detectors, respectively.

$$F_1=\int_{-X_{1\,\min}}^{X_{1\,\max}} d\Omega_1 dx \tag{2}$$

and

$$F_2=\int_{-X_{2\,\min}}^{X_{2\,\max}} d\Omega_1 d\Omega_2 dx, \tag{3}$$

where $d\Omega_i$ is the solid angle subtended by the ith detector at the target position x, $X_{1\,\min}$, and $X_{1\,\max}$ are the limits in the target position observed by a single detector, and $X_{2\,\min}$ and $X_{2\,\max}$ are the target position limits seen by a coincident two-detector system. A numerical integration was carried out over five parallel beam positions within the envelope of the actual beam of 1.5 mm in diameter and the average of these five values was used.

It has been shown[3,10] that the PPB cross section is peaked toward coplanar events by the factor $f(\phi)=1-(\phi/\phi_m)^2$, where $\phi=\phi_1+\phi_2$ and ϕ_m is the maximum kinematically allowed ϕ. In the present experiment, $\phi_m=5.1°$, thus the measured cross section must be increased by 7% to yield the generally calculated coplanar value.

All detector slit diameters were 2.40±0.02 mm as measured with a traveling microscope. The center of the chamber to front and back slit distances were 35.4±0.2 mm and 53.2±0.2 mm, respectively. Incorporating these uncertainties into the calculation of F_1 and F_2 produces an 8% uncertainty in the factor $F=F_1/F_2$. A 5% uncertainty is assigned to the number of elastically scattered protons monitored, N_{el}, because of the error in background subtraction. Less than 1%

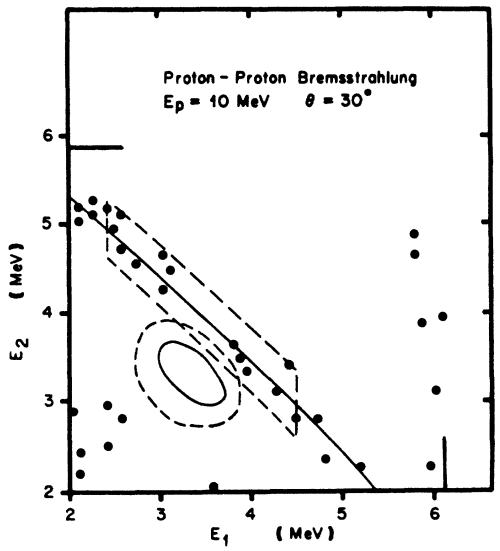

FIG. 4. The PPB kinematics and data at $E_p=10$ MeV, $\theta=30°$. The dots, each representing one count, show the net effect. The solid and dashed curves and lines have the same meaning as in Fig. 3.

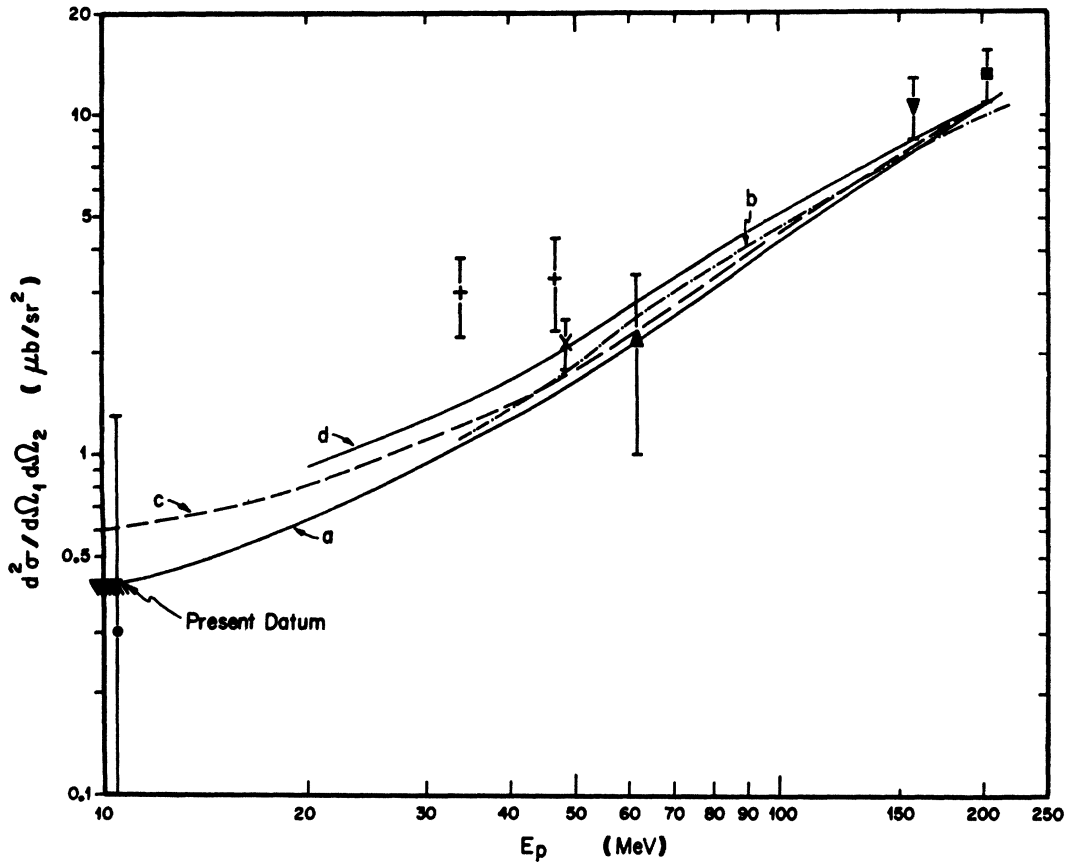

FIG. 5. The present and other data at $\theta=30°$ compared with $\theta=30°$ calculations. a (Ref. 3), b (Ref. 12), c (Ref. 5), d (Ref. 4), ● (Ref. 13), + (Ref. 8), × (Ref. 9), ▲ (Ref. 10), ▼ (Ref. 7), and ■ (Ref. 6).

error is introduced in F due to a 10% error in the beam diameter so that this source of uncertainty can be neglected. Thus the statistical error on N_{PPB} must be increased by a total of 20% in order to obtain an upper limit on the coplanar PPB cross section.

Including the 20% increase discussed above and using 5.5 counts as the upper limit on the yield of PPB events, the upper limit to the PPB cross section as given by Eq. (1) is 0.42 μb/sr^2.

As can be seen from Fig. 5, this upper limit is consistent with the calculation of Pearce and Duck (curve a) and an extrapolation of Nyman's (curve b) result to 10 MeV would approach agreement. However, the result of Signell (curve c) is significantly higher than this upper limit and an extrapolation of Brown's calculation (curve d) also tends to a high value at 10 MeV. It should be emphasized that none of these calculations can be considered exact at 10 MeV since Coulomb interactions have not been included. Introducing the Coulomb interaction would have the effect of reducing the cross section.[17]

Crawley's recently measured value of $0.3(+1.0, -0.3)$ μb/sr^2 at 10.5 MeV and $\theta=30°$ is in agreement with this upper limit of 0.42 μb/sr^2 at 10 MeV, $\theta=30°$.

[17] P. Signell and D. Marker, Phys. Letters **26B**, 559 (1968).